ACS OMEGA

Open Access

http://pubs.acs.org/journal/acsodf

Article

Impact of MTHFD2 Expression in Bladder/Breast Cancer and Screening of Its Potential Inhibitor

Samreen Aruge, Maleeha Asif, Aamira Tariq,* Saaim Asif, Muhammad Zafar, Muhammad Affan Elahi, Lubna Riaz, Aneela Javed, Nazish Bostan, and Sadia Sattar

Cite This: *ACS Omega* 2024, 9, 44193−44202

Read Online

ACCESS | Metrics & More | Article Recommendations | Supporting Information

ABSTRACT: Genes of folate-mediated 1 carbon metabolism are found to be highly upregulated in tumor cells and promote cancer cell proliferation. The current study aimed to determine the expression of the MTHFD2 gene in bladder and breast cancers. Furthermore, the determination of potential ligand-based inhibitors against MTHFD2 was performed in comparison with those of chemotherapeutic drugs and natural plant-based compounds. Semiquantitative expression analysis along with structure-based virtual ligand library screening was done to find plausible inhibitors. MTHFD2 expression was significantly increased with tumor stage progression both in low- and high-grade bladder cancer and especially in triple-negative breast cancer. Virtual ligand-based library screening against the three-dimensional MTHFD2 protein structure led to the identification of plausible inhibitors like MCULE-8109969891-0 and MCULE-9715677418-0-1 that displayed lower binding free energy as compared to that of already documented LY345899. Similar scaffold commercial drugs leucal (LEU), epirubicin (EPI), and lometrexol also displayed strong binding to the active site of MTHFD2. EPI and LEU in combinatorial therapy were also tested in vitro on MDA-MB-231 cells. The high doses of LEU in combination with EPI showed a significant reduction in cell viability at 2 and 3 μM concentrations. The interaction of breast cancer serum with high expression of MTHFD2 also showed an increase in binding of epirubicin in the presence of leucovorin. The decrease in the absorbance spectra of epirubicin at 37 and 53 °C displayed the stability induced by LEU on the interaction of EPI with the MTHFD2 binding pocket. Leucovorin tends to stabilize the interaction as the binding affinity is high even at 53 °C. Thus, MTHFD2 might be used as a cancer biomarker since its expression level changes drastically with tumor progression. Further experimental studies are required to establish the potential mode of inhibition of the novel small ligands. Future in vivo trials may validate the effectiveness of the combinatorial therapy.

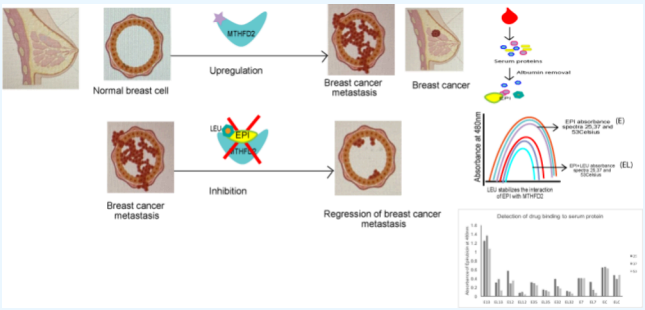

1. INTRODUCTION

In cancerous tissues, the growth and survival of proliferating cells are supported by folate-mediated one-carbon metabolism (FOCM), which acts as the biochemical basis of DNA methylation and nucleotide synthesis.[1] The folate metabolism, which occurs in both cytosol and mitochondria, produces folate intermediates, which drive the upregulation of one carbon (1C) metabolism, thus contributing to the increased expression of several mitochondrial folate pathway enzymes that have been linked to the development of several cancers.[2] The activation and transfer of 1C units for this biosynthesis process aid in purine and thymine synthesis.[3] The methylenetetrahydrofolate dehydrogenase/cyclohydrolase (MTHFD2) is a bifunctional NAD(P)-dependent enzyme that is involved in the mitochondrial folate-mediated one-carbon pathway. MTHFD2 is involved in redox homeostasis by maintaining NADPH, particularly in colorectal cancer cells, and oversees the recycling of tetrahydrofolate (THF) in the mitochondria.[4] It consists of a 350 amino acid residue with 37 kDa molecular weight, which is located exclusively in mitochondria, but recent studies have shown its presence within the nucleus nearer to newly synthesized DNA as well.[5] Its bifunctional cyclohydrolase and dehydrogenase activities promote cellular proliferation, tumor development, and progression. High expression of MTHFD2 has been observed in several cancers including breast cancer,[6] hepatocellular carcinoma,[7] renal cell carcinoma,[8] colorectal cancer,[4] and bladder cancer.[9] Moreover, MTHFD2 inhibition or depletion has been demonstrated to have antiproliferative effects on cancer cells, indicating that it can act as a potentially viable therapeutic target for anticancer drugs and as a prognostic

Received: April 18, 2024
Revised: October 6, 2024
Accepted: October 11, 2024
Published: October 23, 2024

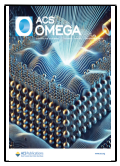

indicator, especially in the case of breast and bladder cancers, whose intensity increases day by day.[5,6]

Breast cancer is among the most common types of cancer in women around the world, which primarily arises in the cells of lobules or milk ducts, whereas bladder cancer is a type of urinary tract cancer that develops from the epithelium lining of the urinary bladder.[10] Both cancers can be metastatic and can spread to distant organs, such as the liver, lungs, brain, and bone, resulting in high mortality rates worldwide. Epirubicin (EPI) is an anthracycline drug used primarily in chemotherapy for the clinical treatment of breast cancer and, in some cases, bladder cancer as well. It exhibits certain side effects including cardiotoxicity due to dose accumulation[11] and damaging healthy organs like the liver, kidney, and brain.[12] Moreover, the respective drug resistance is substantially hindering successful cancer treatments in many cases.[13] Hence, combinational therapy by employing different drugs with EPI can not only enhance its anticancerous activity but also reduce its cytotoxicity. A recent study reported the use of ursolic acid to enhance the activity of EPI resulting in enhanced drug sensitivity of human breast cancer cell lines such as MCF-7 and MDA-MB-231. Furthermore, ursolic acid reduced the clinical dose of EPI in breast cancer patients, thereby decreasing the side effects.[14]

The current study aimed to determine the effect of MTHFD2 overexpression in breast and bladder cancer patients from the Pakistani population. Furthermore, the relationship between MTHFD2 expression and bladder and breast cancer subtypes was established. Using an in silico approach, the MTHFD2 protein was further tested against a pharmacological library from MCULE, and FDA-authorized medications to find possible interacting pharmaceuticals, and then suitable drugs were subjected to in vitro screening on cancer cell lines that may be a promising choice to treat both cancers in patients depicting different expression of the MTHFD2 protein.

2. MATERIALS AND METHODS

2.1. Ethical Approval and Sample Collection. The current study adhered to the principles outlined in the Declaration of Helsinki and was conducted with prior ethical approval from the Pakistan Institute of Medical Sciences (PIMS) Hospital (ECPIMS/19/09/b) and Ethical Review Board (ERB) of COMSATS University Islamabad (CUI), Islamabad, Pakistan (CUI/Bio/ERB/18/76). A total of 40 samples were taken from breast cancer patients, whereas 34 samples were collected from bladder cancer patients, 28 (82.3%) of whom were males and just 6 (17.6%) were females. The patients in the study had an average age of 43.5 ± 16.5 years (range: 17−70 years). A tumor sample of approximately 5 mm in size was taken. As a control, surrounding healthy tissue separated by around 2 cm was obtained from the same patient, as well. All the samples were immediately transferred to RNA latter and were stored in a refrigerator at 2−8 °C.

2.2. MTHFD2 In Silico Analysis. Tissue-specific expression and regulation of MTHFD2 were determined using the Genotype-Tissue Expression database (GTEx database) (https://gtexportal.org/home).[15] Moreover, the GEPIA2 (gene expression profiling interactive analysis) online tool (http://gepia2.cancer-pku.cn/#index) was used to analyze the cancer genome atlas (TCGA) for overall survival and box plots.[16]

2.3. Primer Designing. RNA expression analysis was performed by using exon-spanning primers for targeted genes. The primers were designed by extracting the cDNA sequence of the *MTHFD2* gene (NM_006636.4) from the Ensemble Genome Browser (https://asia.ensembl.org/index.html). Primers were designed using Primer Quest software (https://sg.idtdna.com/pages/tools/primerquest). The designed primers were validated using UCSC in silico PCR (https://genome.ucsc.edu/cgi-bin/hgPcr) and Primer Blast software (https://www.ncbi.nlm.nih.gov/tools/primer-blast/).

2.4. RNA Isolation and Optimization. For RNA isolation, the Trizol reagent method was used with some modifications.[17] A NanoDrop spectrophotometer (Thermo Fisher Scientific, Dover, DE, USA) was used for quantification at A260/280 to ensure the quality of extracted RNA. The cDNA was synthesized by using the RevertAid first-strand cDNA synthesis kit (Thermo Scientific, USA) from the extracted RNA samples[18] by a two-step method. Expression analysis was performed by using the housekeeping gene beta-actin 5′-CTGAACCCCAAGGCCAAC-3′(F) and 5′-AGAGGCGTACATGGGATAG-3′(R) annealed at 59 °C and MTHFD2 primer sequences (5′GATCAAGGAAGGAG-CAGCAG3′(F) and 5′TTCAAGCCTCAG-CACCTTTT3′(R).

2.5. Quantitative Real-Time PCR. Expression analysis was performed using the QuantStudio 7 Pro Real-Time PCR System, 96-well, 0.2 mL (Applied Biosystems, USA) for both the tumor and control samples. The candidate gene's expression was normalized using β-actin (housekeeping gene), and the MTHFD2 gene's expression in tumor breast and bladder samples was compared to that of control samples; real-time analysis was performed using the 2-delta−delta Ct ($2^{-\Delta\Delta Ct}$) method. The normality of the data was tested using the Shapiro−Wilk test, and the outliers were removed using the Grubbs test at the 0.05 level. The significance level of $P < 0.05$ was calculated through Student's t test.

2.6. Virtual Compound Screening against MTHFD2.

2.6.1. Database Preparation. The high-throughput screening library was prepared by combining the Food and Drug Administration (FDA)-approved library from the ZINC (https://zinc.docking.org/) database comprising 1577 drug-like molecules, 1483 molecules from the MCULE Ro5 database (https://mcule.com), and Indian medicinal plants using RASPD$^+$.[19] The unwanted molecules with improper conformation were removed, and charges were assigned to the ligand molecules by using Autodock Vina.

2.6.2. Protein Preparation. The protein was prepared for docking by removing cocrystallized water molecules, non-standard residues and nonpolar hydrogens. Hydrogens and Gasteiger charges were merged. Energy minimization and geometry optimization were performed using the DockPrep built-in tool in UCSF Chimera 10.1 (Resource for Biocomputing, Visualization, and Informatics, University of California San Francisco, San Francisco, CA, USA).[20] The energy was minimized for the 1000 steepest descent steps at a root mean square gradient of 0.02, an update interval of 10, and with an Amber ff12SB force field using UCSF Chimera 10.1. Hydrogens were added to generate protonation states at physiological pH using the energy minimization tool at UCSF Chimera.[20]

2.6.3. Molecular Docking Simulation. Docking simulation was carried out using the PARDOCK$^+$ (http://www.scfbio-iitd.res.in/pardock+/)[21] and fastDRH (http://cadd.zju.edu.cn/fastdrh/) web server[22] employing an Autodock Vina-based docking program. The prepared crystal structure of MTHFD2

https://doi.org/10.1021/acsomega.4c03599
ACS Omega 2024, 9, 44193−44202

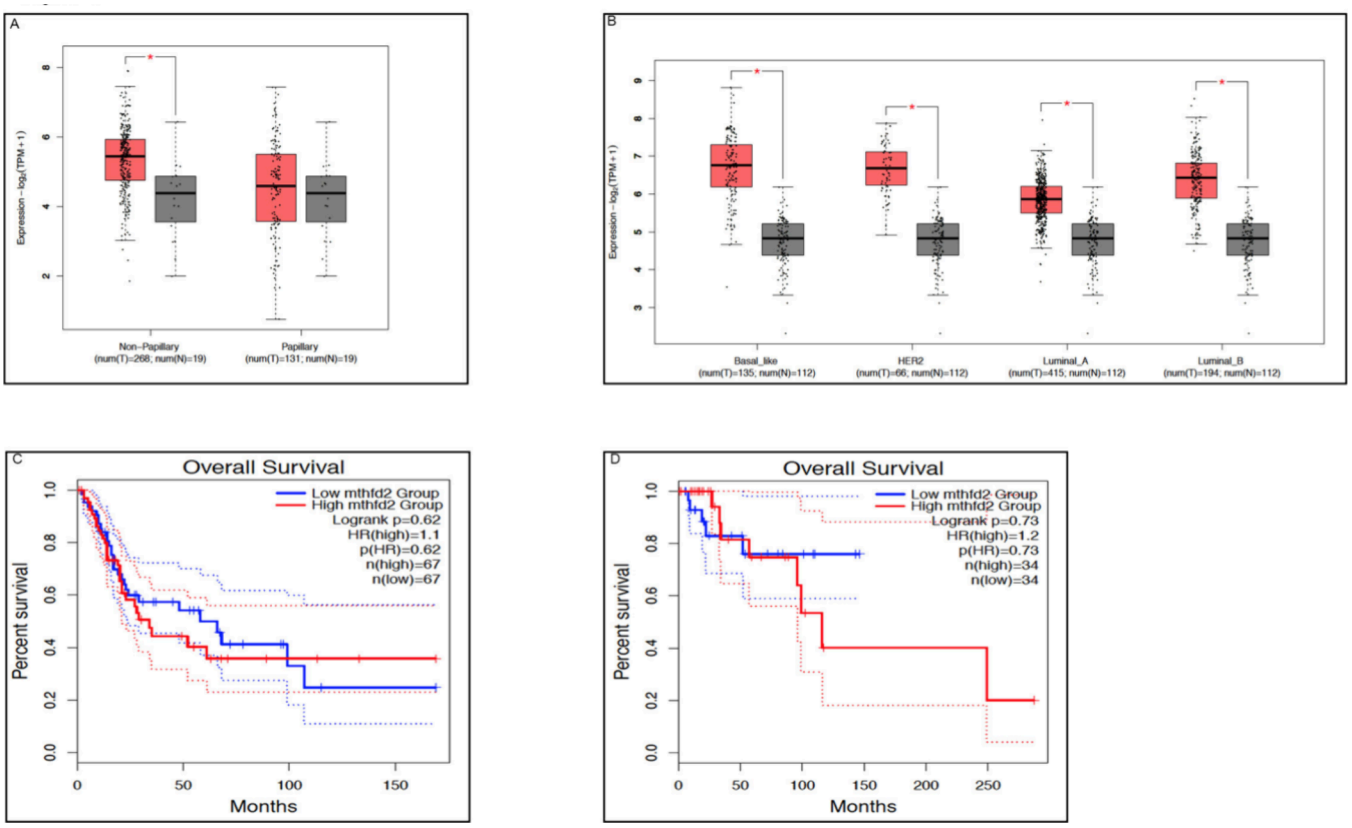

Figure 1. MTHFD2 in silico analysis in bladder and breast cancer. (A) Relative expression analysis of MTHFD2 in bladder cancer molecular subtypes using GEPIA2 analysis software based on the TCGA database using $P \leq 0.05$ as the cutoff criteria. The *Y*-axis represents the log2 (TPM +1) expression values of the respective gene. MTHFD2 showed significant increased expression in nonpapillary subtype of bladder cancer. (B) Relative expression analysis of MTHFD2 in breast cancer molecular subtypes using GEPIA2 analysis software based on the TCGA database using $P \leq 0.05$ as the cutoff criteria. MTHFD2 showed significantly increased expression in all breast cancer subtypes. (C) Survival data indicate that the bladder cancer patients showed significantly reduced disease-free survival in the MTHFD2 high-expression group represented as a red line as compared to the MTHFD2 low-expression group shown in blue. The *X*-axis represents the number of months, and the *Y*-axis shows survival probability. (D) Survival data indicate that triple-negative breast cancer patients showed significantly reduced disease-free survival in the MTHFD2 high-expression group represented as a red line as compared to the MTHFD2 low-expression group shown in blue. The *X*-axis represents the number of months, and the *Y*-axis depicts survival probability.

(5TC4)[5] was used as a receptor. The active site and binding pocket-specific residues were selected for docking. Furthermore, during docking simulations, the top 4 and 9 poses of the compounds were selected. The best docking pose displaying the lowest binding free energy was subjected to Ligplot+ (https://www.ebi.ac.uk/thornton-srv/software/LigPlus/) analysis in order to identify different interactions.

2.7. In Vitro Drug Screening. *2.7.1. Drug Stocks and Dilutions.* A 100 μM stock was prepared by adding 27 μL of EPI (mol wt = 543.5) and 973 μL of DNase/RNase-free water. Different dilutions of EPI ranges from diluted (0.5−1.0 μM) to concentrated (2.0−3.0 μM) were prepared in complete media (90% DMEM, 10% FBS, and 1% pen/strep). A leucovorin calcium (LEU mol wt = 573) 100 μM stock was prepared by mixing 17.2 μL from the stock and 982.8 μL of DNase/RNase-free water. Different dilutions of LEU 2.5, 5.0, 10, 20, and 40 μM were prepared. The cytotoxicity in breast cancer cells was analyzed by using EPI and LEU alone and in combination at different concentrations.

2.7.2. Cell Viability Assay. The breast cancer cell line MDA-MB-231 was cultured in Dulbecco's modified Eagle's medium (DMEM) supplemented with 10% fetal bovine serum (FBS) and 1% penicillin/streptomycin (Thermo Fisher Scientific, Waltham, MA, USA). Exponentially growing cells were counted using a hemocytometer, and 10,000 cells were seeded per well in triplicate in flat-bottom 96 well plates (Nunc, Roskilde, Denmark) and incubated at 37 °C in an atmosphere of 5% CO_2 supply for 24 h. After 24 h of treatment, the cells were observed under a microscope, the drug media was discarded, and fresh media was administered. 15 μL of MTT (3-[4,5-dimethylthiazol-2-yl]-2,5-diphenyltetrazolium bromide) (Sigma-Aldrich, St. Louis, MO, USA) dye was added to each well, and the plate was incubated for 3 h. After incubation, all the media and dye were discarded, and 100 μL of DMSO was added and left for 30 min to dissolve the intracellular purple formazan crystals. Finally, the absorbance of the cells was measured by a spectrophotometer at 550 nm. After measurements were performed, the concentration required for a 50% inhibitory concentration (IC50) was determined graphically. A standard graph was plotted by taking the concentration of the drug on the *X*-axis and relative cell viability on the *Y*-axis.

$$\text{Cell viability (\%)} = \text{Mean OD/Control OD} \times 100\%$$

2.8. Evaluation of Drug Target Interaction. *2.8.1. Albumin Removal Protocol from Serum.* Serum albumin was removed by treating 200 μL of the sample with 2 mL of 1% trichloroacetic acid (1% TCA) in ice-cold isopropanol and

https://doi.org/10.1021/acsomega.4c03599
ACS Omega 2024, 9, 44193−44202

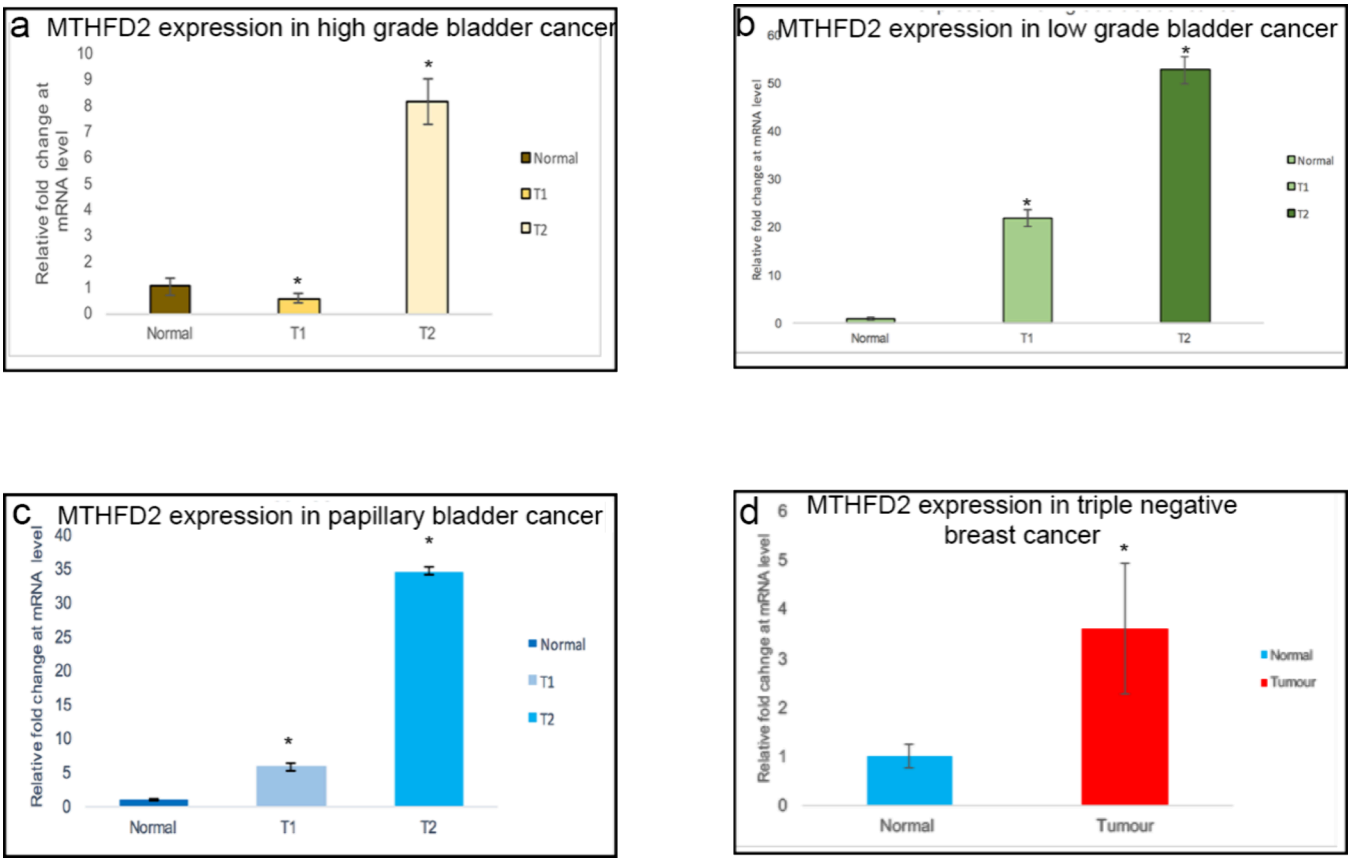

Figure 2. Expression analysis of MTHFD2 in bladder cancer. (a) High-grade bladder cancer. (b) Low-grade bladder cancer. (c) Papillary bladder cancer. (d) Expression analysis of MTHFD2 in triple-negative breast cancer. (a–d) represent ±SD of three independent experiments, i.e., biological replicates. *P*-values (*$P < 0.05$, **$P < 0.01$) were obtained by using Student's *t* test.

vortexing it for 2 min followed by centrifugation at 4000 rpm for 5 min. The supernatant was discarded, and the pellets were washed twice with 2 mL of methanol by centrifugation at 2000 rpm for 2 min. The pellets were resuspended in 2 mL of ice-cold PBS.

2.8.2. Evaluation of Drug Target Interaction with Albumin-Free Serum Proteins. Albumin-free serum proteins of patient and control samples were treated with 3 μM epirubicin, 40 μM leucovorin, and a combination of 3 μM epirubicin and 40 μM leucovorin and incubated at 4 °C for 2 h. After incubation, the samples were given a thermal shift at 25, 37, and 53 °C for 8 min, and absorbance was taken at 500 nm.

2.9. Statistical Analysis. GraphPad Prism 8.0 software (San Diego, CA, USA) was used to calculate the statistical significance. All data were provided as means and SEM. Student's *t* test was used for determining statistical significance. Values below the *P* value of 0.05 were considered significant.

3. RESULTS

3.1. In Silico Analysis of MTHFD2 Expression. MTHFD2 expression was examined using TCGA data sets for both bladder and breast cancer along with their subtypes. Bladder cancer is subdivided into papillary and nonpapillary subtypes, whereas breast cancer is subdivided into Luminal A, Luminal B, HER2, and TNBC subtypes. MTHFD2 was shown to be significantly upregulated in nonpapillary bladder carcinomas as compared to normal samples (Figure 1a). MTHFD2 showed significant upregulation in different breast cancer subtypes (Figure 1b). However, the strongest upregulation of MTHFD2 was observed in the basal subtype (Figure 1b). Disease-free patient survival analysis revealed that the high-expression group (shown in red) had a lower survival probability, whereas the low-expression group (shown in blue) had a better survival probability. However, after 100 months, the survival probability of the high-expression group increased in nonpapillary bladder cancer (Figure 1c). A strong decline in patient disease-free survival analysis has been observed in the case of the MTHFD2 high-expression group (Figure 1d), demonstrating its predominant oncogenic potential, especially in breast cancer.

3.2. Expression Analysis of MTHFD2. The significant upregulation in both breast and bladder cancer via an in silico study was further validated in patient samples. In nonpapillary cancers, samples from both low and high grades were taken. The relative expression analysis showed significantly high expression in both low- and high-grade bladder cancers. Expression was low in the high-grade T1 stage compared to controls (Figure 2a); however, in the T2 stage, there was a significant 8-fold rise at the mRNA level (Figure 2a). On the contrary, both T1 and T2 stages of low-grade bladder cancer showed a significant increase in MTHFD2 expression (Figure 2b). suggesting the role of MTHFD2 in low-grade malignancy progression. In the case of papillary bladder cancer, a significant increase in MTHFD2 expression (approximately 5- and 34-fold) was observed, showing its profound impact on less invasive bladder cancer subtypes (Figure 2c). Contrastingly, in the basal breast cancer subtype (i.e., the most

https://doi.org/10.1021/acsomega.4c03599
ACS Omega 2024, 9, 44193−44202

aggressive subtype of breast cancer), a 5-fold increase (Figure 2d) was observed, indicating that the expression shows variation among different subtypes and tissue types.

3.3. Structure-Based Virtual Screening. The 3D crystal structure of MTHFD2 was resolved with inhibitors like LY345899[5] (PDB ID 5TC4). The affinity of MTHFD2 to this inhibitor was mainly due to the presence of the binding pocket that harbors interacting residues (SER 83, TYR 84, ASN 87, LYS 88, LEU 130, VAL 131, GLN 132, LEU 133, PRO 134, ASP 155, GLY 156, PHE 157, ALA 175, THR 176, ILE 276, ASN 277, ARG 278, LEU 289, PRO 309, GLY 310, GLY 311, VAL 312, GLY 313, PRO 314, MET 315, THR 316, and VAL 317). The virtual screening library was compiled by combining the ZINC FDA-approved drug library MCULE Ro5 and the Indian medicinal plant library to find new drug-based inhibitors against MTHFD2 (PDB ID 5TC4). Between 4 and 10 different conformations for each ligand were generated using PARDOCK$^+$ and fastDRH. These ligand-based interactions were then classified based on docking scores. The top 7 ranked compounds displaying the best docking scores are presented in Table 1, and the Indian medicinal plant-based compounds with the best docking scores are listed in Table 2. The most stable docking complex was of MCULE-9715677418-0-1 (docking score = −10.93 and −11.4) followed by MCULE-8109969891-0 (docking score = −11.3 and −9.4) (Table 1, Supplementary Figures S1 and S2). Three commercially available drugs (leucal (LEU, calcium folinate), EPI, and lometrexol) that resembled closely with the two best docked complexes were chosen for interaction analysis with MTHFD2. Docking analysis revealed that LEU and EPI (docking score = (−10.12, 9.3) and (−9.67, −10.535), respectively) can bind efficiently with MTHFD2 (5TC4) (Table 1, Supplementary Figures S1 and S2).

Table 1. Docking Score Generated by Pardock+ and fastDRH against the Ligand Library

sr. no.	ligand	docking score Pardock+	docking score fastDRH
1	MCULE-9715677418-0-1	−10.93	−11.438
2	MCULE-8109969891-0	−11.3	−9.453
3	MCULE-6777136947 (LY345899)	−10.48	−9.763
4	MCULE-8042763540-1 (lometrexol)	−10.51	−9.286
5	MCULE-6876833663-1 (leucal)	−10.12	−9.308
6	MCULE-3376329397-0	−10.36	−8.904
7	MCULE-9735088477-0 (epirubicin)	−9.67	−10.535
8	MCULE-2077919807-2	−9.51	−9.377

Table 2. Docking Score Generated by Pardock+ and fastDRH against the Indian Medicinal Plant-Derived Compounds

sr. no.	ligand	docking score Pardock+	docking score fastDRH
1	IMPHY011337 (Grossamide)	−9.34	−9.67
2	IMPHY001562 (Cannabisin a)	−9.23	−9.49
3	IMPHY003169 (6-deoxocastasterone)	−9.23	−6.71

The Ligplot analysis of PARDOCK$^+$ based docking poses of the two most stable docking complexes revealed that MCULE-9715677418-0-1 (docking score = −10.93) and MCULE-8109969891-0 (docking score = −11.3) along with LY345899 (MCULE-6777136947) interacted well as shown in Figure 3. MCULE-8109969891-0 established multiple hydrogen bonds with the oxygen atoms of Asp238, Pro267, and Asp120. The oxygen atoms of the potential inhibitor were engaged in hydrogen bonding with the hydrogen atoms of Gln97, Thr141, Ala140, and Lys53 (Figure 3). Moreover, different hydrophobic interactions were seen with different residues at the active site of MTHFD2. MCULE-9715677418-0-1 being an aromatic molecule interacted hydrophobically with Arg55, Asn52, Val277, Gly273, Ile241, Pro274, Tyr49, Leu98, Gln97, and Pro99 (Figure 3).

Ligplot-based analysis of MCULE-6876833663-1 (leucal) revealed two hydrogen bonds between the oxygen atoms of Asp120 and the drug molecule. Another hydrogen binding was found between the Asn52 hydrogen atom and the oxygen atom of the drug molecule. Apart from this, different amino acids such as Phe122, Ala140, Thr141, Thr276, Val277, Lys53, Gln97, and Tyr49 were engaged in hydrophobic interaction with the ligand. Epirubicin interacted through hydrogen bonding with Ala218, Ala219, Asn169, Tyr49, and Thr141 of the MTHFD2 active site, validating its strong binding. Lometrexol was engaged in three different hydrogen bonds with Thr141, Asn19, and Thr276. Thus, the binding of these three drug molecules is comparable to that of the previously reported inhibitor LY34. Furthermore, the RASPD tool was used to find natural compounds that could bind efficiently with the active site of MTHFD2. Three different plant-based compounds were shortlisted based on a good docking score (Table 2). IMPHY011337 (Grossamide) and IMPHY001562 (Cannabisin a) displayed good docking scores in comparison with LY34.

Ligplot analysis revealed that IMPHY011337 interacted most hydrophobically with the MTHFD2 active site. Two hydrogen bond-based interactions were observed between the hydrogen atoms of Gly270, Arg243, and the oxygen atoms of IMPHY011337, whereas IMPHY001562 interacted hydrophobically with the LY34 binding site of MTHFD2 except one hydrogen bond between Asp120 and the drug molecule (Supplementary Figures S3 and S4).

3.4. Prediction of ADMET Properties. Molecular descriptors are critical factors to determine the pharmacokinetic properties and toxicity of the candidate compounds. In silico ADMET property prediction aids in identifying the potential therapeutic compounds. The BBB, aqueous solubility, CYP450 inhibition, Lipinski rule violation, and PAIN evaluation for toxicity determination were used for screening for potential ADMET properties predicted. Supplementary Tables 1−3 depict the structural characteristics and the ADMET profiles of the selected ligands.

3.5. Cell Viability Analysis. *3.5.1. Effect of EPI and LEU on Cell Viability.* The docking scores evaluated by PARDOCK$^+$ and fastDRH for leucal and EPI were comparable to those of the already established ligand LY34. EPI is an anthracycline drug with restricted usage owing to its adverse side effects at high doses.[23] Therefore, a combinatorial therapy is required that can effectively reduce the effective concentration. The cytotoxic effect of EPI alone and in combination with LEU was determined. The IC50 graphs are depicted in Supplementary Figure S5.

https://doi.org/10.1021/acsomega.4c03599
ACS Omega 2024, 9, 44193−44202

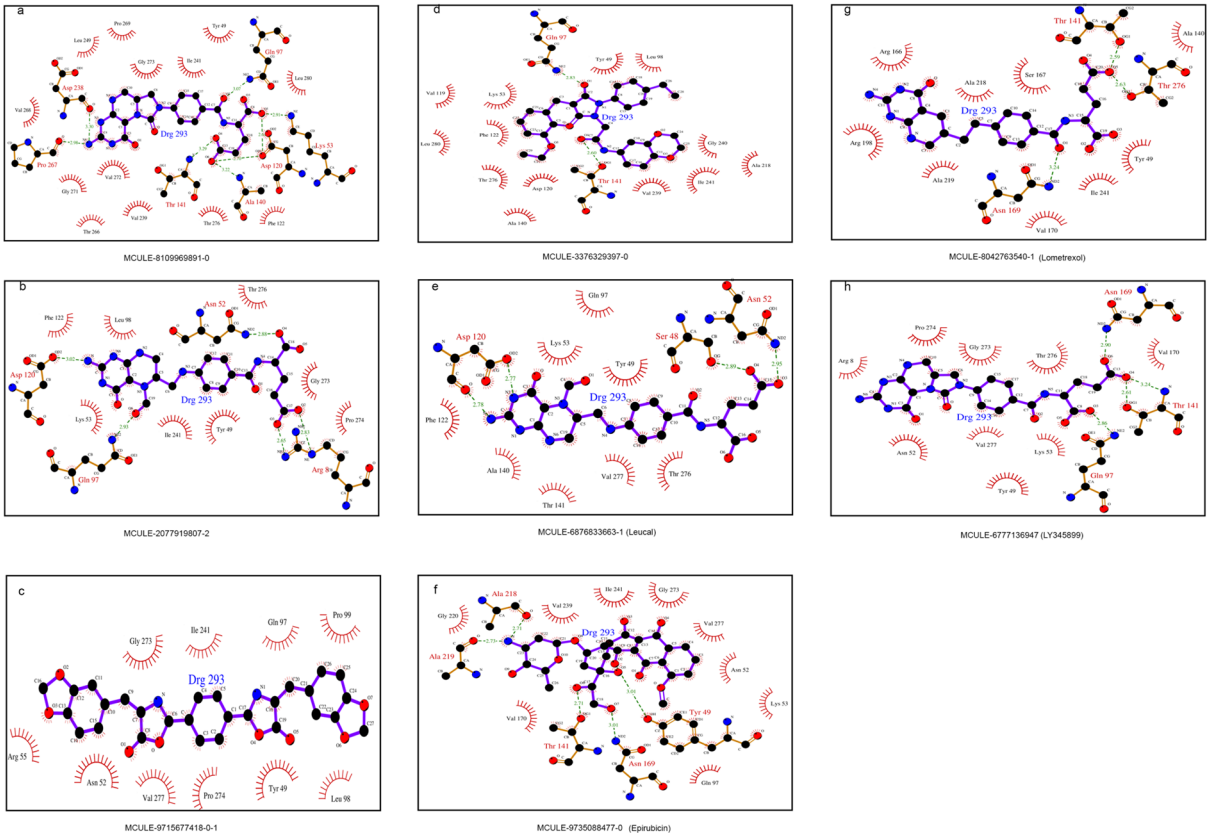

Figure 3. Ligplot+ based interaction analysis of the MTHFD2 structure (5TC4) and ligand docked complexes: (A) MCULE-8109969891-0, (B) MCULE-2077919807-2, (C) MCULE-9715677418-0-1, (D) MCULE-3376329397-0, (E) MCULE-6876833663-1 (leucal), (F) MCULE-9735088477-0 (epirubicin), (G) MCULE-8042763540-1 (lometrexol), and (H) MCULE-6777136947 (LY345899). Green dashed lines indicate hydrogen bonds with distance in angstrom (Å), spoked red arcs indicate hydrophobic contacts, atoms are shown in black for carbon, blue for nitrogen, red represents oxygen, and yellow represents sulfur. (C) MCULE-9715677418-0-1 showed hydrophobic interactions, whereas (A) MCULE-8109969891-0 exhibited multiple hydrogen bonding and hydrophobic interactions with the binding pocket of MTHFD2.

The effect of EPI and LEU alone and in different combinations on breast cancer cell proliferation was also determined by estimating the cell survival percentages at different concentrations. Results showed that EPI dramatically reduced the cell proliferation after 24 h in a concentration-dependent manner (Figure 4a). The cell viability is reduced to 40% at 3 μM EPI dosage. Although EPI is a potent chemotherapeutic drug, its adverse effects limit its usage and efficacy. LEU, on the other hand, showed an increase in cell survival with an increase in drug dosage. The cell viability was reduced to 85.6% at a low dosage of 2.5 μM, but at high doses around 40 μM, the cell viability increased to 99.1% (Figure 4b).

3.5.2. Effect of LEU on the Sensitivity of MDA-MB-231 Cell Lines to EPI. The effect of the combinatorial therapy of LEU and EPI was evaluated on MDA-MB-231 cells. A minimal decrease in cell viability was observed in the case of combined therapy of 0.5 μM and 1.0 μM EPI with all respective concentrations of LEU as shown in Figure 4c,d (Supporting Tables S4−S7). However, a significant decrease in cell proliferation was observed at 2.0 μM EPI with 10, 20, and 40 μM LEU concentrations from 45.9, 41.75, and 38.25%, respectively as compared to 2 μM EPI alone with cell viability around 48.9% (Supporting Tables S8 and S9). This inhibition increased and viability decreased when LEU different concentrations were administered with 3.0 μM EPI from 36.32 to 34.55% as compared to 3.0 μM EPI dosage exhibiting 41% cell viability (Figure 4e,f, Supporting Tables S10 and S11).

3.5.3. Effect of Drug Interaction with Serum Proteins. Serum albumin was removed, and the remaining serum proteins were exposed to different temperatures (25, 37, and 53 °C) in the presence of epirubicin alone and epirubicin along with leucovorin. Epirubicin displayed maximum absorbance at 480 nm. Breast cancer patient serum samples were treated with epirubicin (E) and epirubicin along with leucovorin (EL). The stability of the binding was assessed at different temperatures. Interestingly, in the presence of leucovorin, a strong decrease in epirubicin absorbance at 480 nm was observed plausibly due to its binding with the serum proteins. However, a lesser decrease was observed in the case of control samples (EC and ELC). A prominent decrease in fluorescence was observed at 37 and 53 °C, indicating the stability of the complex (Figure 5 and Supporting Table S12).

4. DISCUSSION

Cancer is a complex disease characterized by uncontrolled cell growth and survival. Moreover, cancer and normal cells differ greatly with respect to cellular metabolism.[24] Understanding the specific mechanisms underlying cancer cell metabolism has been an area of intense research as it offers potential insights into developing targeted therapies. One particular focus has been on MTHFD2, a key enzyme involved in cancer cell-specific metabolism. The overexpression of MTHFD2 has

https://doi.org/10.1021/acsomega.4c03599
ACS Omega 2024, 9, 44193−44202

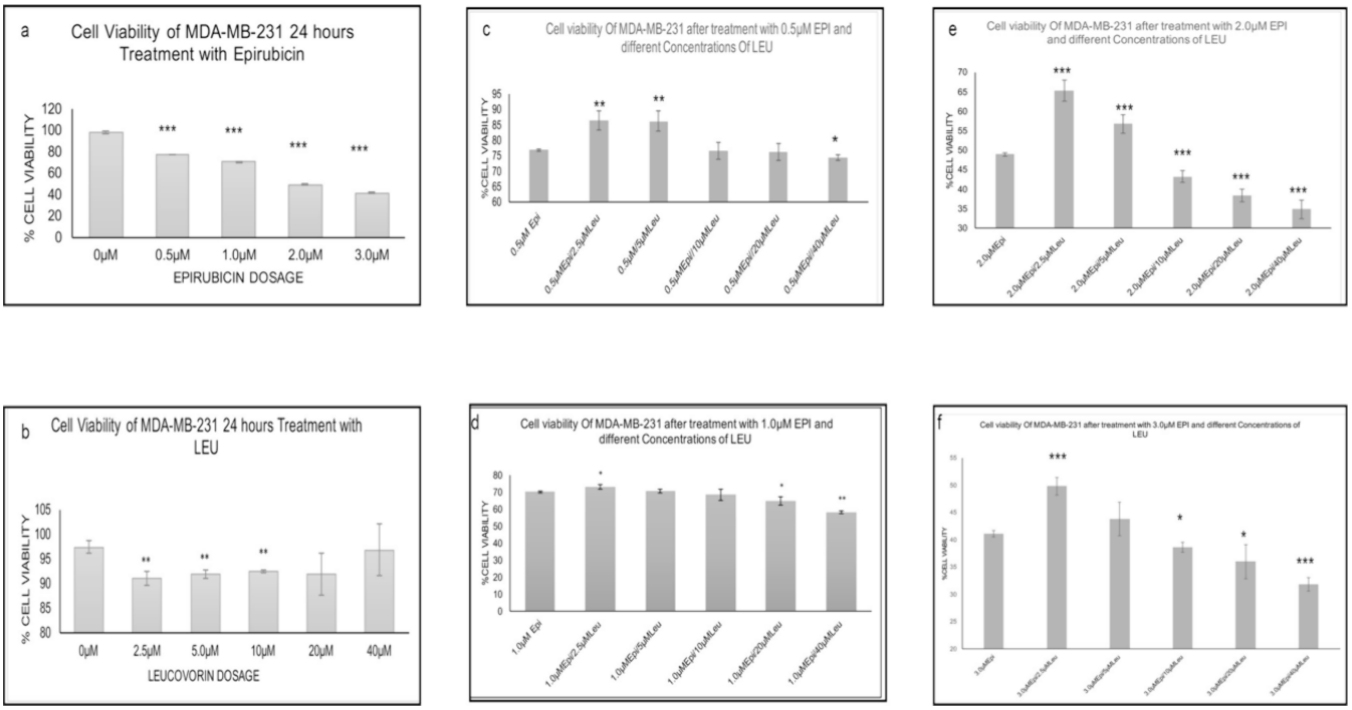

Figure 4. Effect of epirubicin and/or leucovorin on the viability of MDA-MB-231 cells. (a) Decrease in the cell viability percentage on increasing dosage of epirubicin treatment of MDA-MB231 cells. (b) Decrease in cell viability percentage at low doses of leucovorin (LEU) treatment (2.5−10 μM concentration), whereas an increase in cell viability was observed at 20 and 40 μM concentrations. (c) Significant increase in cell viability was observed on treatment of MDA-MB231 cells at 0.5 μM epirubicin in combination with 2.5 and 5 μM LEU concentrations. No significant change in cell viability was observed at 0.5 μM epirubicin in combination with 10, 20, and 40 μM LEU concentrations. (d) Significant increase in cell viability was observed on treatment of MDA-MB231 cells at 1 μM epirubicin in combination with 2.5 μM LEU concentration. No significant change in cell viability was observed at 1 μM epirubicin in combination with 5 and 10 μM LEU concentrations. Significant decrease in cell viability was observed on treatment of MDA-MB231 cells at 1 μM epirubicin in combination with 20 and 40 μM concentrations of LEU. (e) Significant increase in cell viability was observed on treatment of MDA-MB231 cells at 2 μM epirubicin in combination with 2.5 μM LEU concentration. Significant decrease in cell viability was observed on treatment of MDA-MB231 cells at 2 μM epirubicin in combination with 5, 10, 20, and 40 μM concentrations of LEU. (f) Significant increase in cell viability was observed on treatment of MDA-MB231 cells at 3 μM epirubicin in combination with 2.5 μM LEU concentration. Significant decrease in cell viability was observed on treatment of MDA-MB231 cells at 3 μM epirubicin in combination with 10, 20, and 40 μM concentrations of LEU. (a−d) represent ±SD of three independent experiments, i.e., biological replicates. *P*-values (*P < 0.05, **P < 0.01, ***P < 0.001) were obtained by using Student's t test.

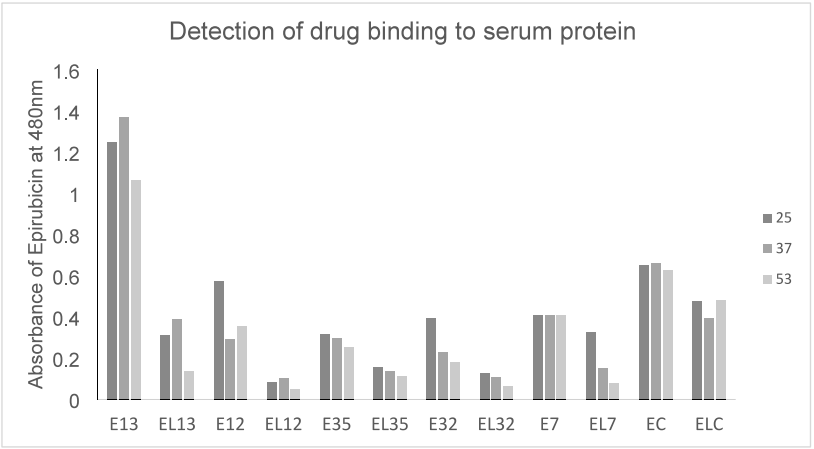

Figure 5. Bar graph showing the enhanced binding of epirubicin to serum proteins in the presence of leucovorin.

been observed in many types of cancer,[25,26] making it a potential target for drug development. Furthermore, the link between high hypoxia levels and MTHFD2[27] emphasizes its significance in the context of cancer progression. Thus, targeting MTHFD2 has the potential to disrupt the metabolic reprogramming of cancer cells, leading to decreased tumor growth and improved patient outcomes. With the increasing prevalence of cancer worldwide, the search for novel compounds with potential therapeutic efficacy has become a key focus in the field of oncology. The exploration of natural compounds, synthetic molecules, and biologically derived substances has unveiled a vast array of potential candidates

https://doi.org/10.1021/acsomega.4c03599
ACS Omega 2024, 9, 44193−44202

for cancer therapy. These compounds exhibit diverse mechanisms of action, targeting specific pathways and molecular processes implicated in tumorigenesis and cancer progression. TCGA-based data analysis revealed significant upregulation of MTHFD2 in nonpapillary bladder cancer and breast cancer subtypes. The high-expression group also displayed a low survival probability TCGA data set. In the present study, the expression analysis of MTHFD2 was done in different bladder and breast cancer subtypes. Structure-based virtual screening in comparison to the already documented inhibitor LY34[5] revealed two plausible inhibitors (MCULE-9715677418-0-1 and MCULE-8109969891-0) of MTHFD2. These compounds displayed low toxicity at the cellular and tissue levels, indicating their potential as novel MTHFD2 inhibitors. Apart from these novel candidates, three drugs LEU, EPI, and lometrexol showed good docking interactions with MTHFD2. EPI is an anthracycline drug that blocks DNA synthesis via intercalation into DNA. The applications of EPI are limited owing to its adverse side effects like dosage-related cardiotoxicity.[23] Leucal is a folate analogue widely used as an antineoplastic and to counteract the toxic effects of folate antagonists.[28] It is mainly used to counteract the toxicity induced by folate inhibitors like methotrexate.[29] LEU and EPI displaying good docking interactions with the LY34 binding pocket of 5tc4 were tested for their impact on cell viability. Interestingly, a 13, 14, and 10% decrease in cell viability was observed when 40 μM LEU was used along with 1, 2, and 3 μM EPI, respectively, as compared to EPI alone (1, 2, and 3 μM) indicating its potential to be used as a combinatorial therapy. A previous study has documented a combinatorial therapy of ursolic acid (20 μM) and EPI (5 μM) reducing the MDA-MB231 cell viability to approximately 34%.[14] In the current study, a strong decrease in cell viability (34 and 31%, respectively) was observed at 2 and 3 μM EPI concentrations in combination with 40 μM LEU. The effectiveness of this therapy can be postulated based on their docking interaction with the MTHFD2 active site. Moreover, leucovorin increased the interaction of epirubicin with serum proteins and seems to have a stabilizing effect.

Apart from this, two compounds (IMPHY011337 and IMPHY001562) based on Indian medicinal plants showed strong interactions with the active site of MTHFD2 (Table 2). IMPHY011337 and IMPHY001562 belong to the class of phenyl propanoids and neolignan-like compounds. The lack of availability of (MCULE-9715677418-0-1 and MCULE-8109969891-0, IMPHY011337 and IMPHY001562) has restricted their evaluation at the cellular level in the current study. Therefore, there is a high probability that these novel compounds can also act effectively to reduce cancer progression.

However, future pharmacological studies are required to determine its optimal inhibitory concentration in cancer cells and mode of inhibition to elucidate the molecular mechanism of action. Understanding how these compounds interact with MTHFD2 at a structural and functional level will provide valuable insights into their potential as targeted therapeutics. Moreover, understanding the selectivity profile of these inhibitors will be instrumental in determining their suitability for further development as targeted treatments for MTHFD2-associated diseases.

5. CONCLUSIONS

In this study, the expression of genes related to the mitochondrial folate pathway such as MTHFD2 was investigated in bladder and breast cancer. MTHFD2 is highly expressed in the low-grade bladder tumor stages and triple-negative breast cancer. The virtual ligand-based screening against MTHFD2 leads to potential inhibitors with low binding energy as compared to the LY34 already documented ligand. Moreover, combinatorial therapy was found to be effective at low doses of EPI overcoming its dosage-specific toxicity. However, future studies are required to determine the potential inhibitor mode of action.

■ ASSOCIATED CONTENT

Supporting Information

The Supporting Information is available free of charge at https://pubs.acs.org/doi/10.1021/acsomega.4c03599.

Best docking poses of ligands generated by PARDOCK+ with lowest binding free energy; best docking poses of ligands generated by fastDRH with lowest binding free energy; docking poses of plant-based compounds generated by PARDOCK+ and fastDRH; Ligplot+ based interaction analysis of the MTHFD2 structure (5TC4) and plant-based ligands docked complexes; IC50 graphs of epirubicin and leucovorin showing increase in cell toxicity with the increase in concentration of epirubicin, whereas in leucovorin increase in concentration decreases the cell toxicity percentage; structural characteristics of ligands; structural characteristics of ligands derived from Indian medicinal plants; ADMET table of the ligands; effect of 0.5 μM epirubicin without and with leucovorin; cumulative effect of 0.5 μM epirubicin without and with leucovorin; effect of 1.0 μM epirubicin without and with leucovorin; cumulative effect of 0.5 μM epirubicin without and with leucovorin; effect of 2.0 μM epirubicin without and with leucovorin; cumulative effect of 2.0 μM epirubicin without and with leucovorin; cumulative effect of 3.0 μM epirubicin without and with leucovorin; cumulative effect of 3.0 μM epirubicin without and with leucovorin; and the effect of different temperatures on binding of epirubicin (E) without and with leucovorin (EL) (PDF)

■ AUTHOR INFORMATION

Corresponding Author

Aamira Tariq − *Department of Biosciences, COMSATS University Islamabad, 45550 Islamabad, Pakistan;* orcid.org/0000-0003-3962-3320; Email: aamira_tariq@comsats.edu.pk

Authors

Samreen Aruge − *Department of Biosciences, COMSATS University Islamabad, 45550 Islamabad, Pakistan*

Maleeha Asif − *Department of Biochemistry, Hazara University, Mansehra, Khyber Pakthunkhwa 21120, Pakistan*

Saaim Asif − *Department of Biosciences, COMSATS University Islamabad, 45550 Islamabad, Pakistan*

Muhammad Zafar − *Institute of Kidney Disease, Peshawar, Khyber Pakthunkhwa 25100, Pakistan*

Muhammad Affan Elahi − *Department of Biochemistry and Molecular Medicine, College of Medicine, Alfaisal University, Riyadh 11533, Saudi Arabia*

https://doi.org/10.1021/acsomega.4c03599
ACS Omega 2024, 9, 44193−44202

Lubna Riaz − *Micro-molecular lab, Public Health Laboratories Division, National Institute of Health, 45500 Islamabad, Pakistan*

Aneela Javed − *ASAB, NUST University, Islamabad 44000, Pakistan;* orcid.org/0000-0003-0280-0610

Nazish Bostan − *Molecular Virology Laboratories, Department of Biosciences, COMSATS University Islamabad, Islamabad 45550, Pakistan;* orcid.org/0000-0003-2226-5440

Sadia Sattar − *Molecular Virology Laboratories, Department of Biosciences, COMSATS University Islamabad, Islamabad 45550, Pakistan*

Complete contact information is available at: https://pubs.acs.org/10.1021/acsomega.4c03599

Author Contributions

S.A. and M.A. contributed equally to this work. A.T. conceptualized and supervised the research and manuscript preparation. M.A. performed the bladder cancer work, and S.A. was involved in the breast cancer work. S.A. and A.J. performed the in vitro studies. S.A. carried out the in silico work along with M.A.E. M.Z. facilitated the sample collection. L.R. and A.J. facilitated the qPCR and cell culture studies. S.A. and N.B. have critically reviewed and edited the manuscript

Funding

This research did not receive any specific grant from funding agencies in the public, commercial, or not-for-profit sectors. However, the cell culture experiments were funded by the grant received by A.T. (8335/Federal/NRPU/R&D/HEC/2017) from the Higher Education Commission of Pakistan under the HEC-NRPU program.

Notes

The study was approved by the Ethical Review Board of COMSATS University Islamabad, Islamabad Campus, Pakistan (approval no. CUI/Bio/ERB/18/76) and Pakistan Institute of Medical Sciences (PIMS) Hospital (ECPIMS/19/09/b).

The authors declare no competing financial interest.

■ ACKNOWLEDGMENTS

We thank Dr. Liaquat Ali (Institute of Kidney Disease, Hayatabad Medical Complex, Hayatabad, Peshawar) for his support for this study. Special thanks to the Surgical department medical team and Histology department (PIMS Hospital, Islamabad) and Molecular Biology Lab (NIH, Islamabad) for their support and sampling.

■ REFERENCES

(1) Tibbetts, A. S.; Appling, D. R. Compartmentalization of Mammalian folate-mediated one-carbon metabolism. *Annual review of nutrition* **2010**, *30*, 57−81.

(2) Yang, M.; Vousden, K. H. Serine and one-carbon metabolism in cancer. *Nature Reviews Cancer* **2016**, *16* (10), 650−662.

(3) Ducker, G. S.; Rabinowitz, J. D. One-carbon metabolism in health and disease. *Cell metabolism* **2017**, *25* (1), 27−42.

(4) Ju, H.-Q.; Lu, Y.-X.; Chen, D.-L.; Zuo, Z.-X.; Liu, Z.-X.; Wu, Q.-N.; Mo, H.-Y.; Wang, Z.-X.; Wang, D.-S.; Pu, H.-Y. Modulation of redox homeostasis by inhibition of MTHFD2 in colorectal cancer: mechanisms and therapeutic implications. *JNCI, J. Natl. Cancer Inst.* **2019**, *111* (6), 584−596.

(5) Gustafsson, R.; Jemth, A.-S.; Gustafsson, N. M.; Färnegårdh, K.; Loseva, O.; Wiita, E.; Bonagas, N.; Dahllund, L.; Llona-Minguez, S.; Häggblad, M. Crystal structure of the emerging cancer target MTHFD2 in complex with a substrate-based inhibitor. *Cancer Res.* **2017**, *77* (4), 937−948.

(6) Liu, F.; Liu, Y.; He, C.; Tao, L.; He, X.; Song, H.; Zhang, G. Increased MTHFD2 expression is associated with poor prognosis in breast cancer. *Tumor Biology* **2014**, *35*, 8685−8690.

(7) Liu, X.; Huang, Y.; Jiang, C.; Ou, H.; Guo, B.; Liao, H.; Li, X.; Yang, D. Methylenetetrahydrofolate dehydrogenase 2 overexpression is associated with tumor aggressiveness and poor prognosis in hepatocellular carcinoma. *Digestive and Liver Disease* **2016**, *48* (8), 953−960.

(8) Lin, H.; Huang, B.; Wang, H.; Liu, X.; Hong, Y.; Qiu, S.; Zheng, J. MTHFD2 overexpression predicts poor prognosis in renal cell carcinoma and is associated with cell proliferation and vimentin-modulated migration and invasion. *Cellular Physiology and Biochemistry* **2018**, *51* (2), 991−1000.

(9) Andrew, A. S.; Gui, J.; Sanderson, A. C.; Mason, R. A.; Morlock, E. V.; Schned, A. R.; Kelsey, K. T.; Marsit, C. J.; Moore, J. H.; Karagas, M. R. Bladder cancer SNP panel predicts susceptibility and survival. *Human genetics* **2009**, *125*, 527−539.

(10) Oliveira, A. I.; Jerónimo, C.; Henrique, R. Moving forward in bladder cancer detection and diagnosis: the role of epigenetic biomarkers. *Expert Review of Molecular Diagnostics* **2012**, *12* (8), 871−878.

(11) Rahman, A. M.; Yusuf, S. W.; Ewer, M. S. Anthracycline-induced cardiotoxicity and the cardiac-sparing effect of liposomal formulation. *Int. J. Nanomed.* **2007**, *2* (4), 567−583.

(12) Marinello, J.; Delcuratolo, M.; Capranico, G. Anthracyclines as topoisomerase II poisons: from early studies to new perspectives. *International journal of molecular sciences* **2018**, *19* (11), 3480.

(13) Sun, W.-L.; Chen, J.; Wang, Y.-P.; Zheng, H. Autophagy protects breast cancer cells from epirubicin-induced apoptosis and facilitates epirubicin-resistance development. *Autophagy* **2011**, *7* (9), 1035−1044.

(14) Wang, Z.; Zhang, P.; Jiang, H.; Sun, B.; Luo, H.; Jia, A. Ursolic Acid Enhances the Sensitivity of MCF-7 and MDA-MB-231 Cells to Epirubicin by Modulating the Autophagy Pathway. *Molecules* **2022**, *27* (11), 3399.

(15) Tung, K.-F.; Pan, C.-Y.; Chen, C.-H.; Lin, W.-C. Top-ranked expressed gene transcripts of human protein-coding genes investigated with GTEx dataset. *Sci. Rep.* **2020**, *10*, 16245.

(16) Tang, Z.; Li, C.; Kang, B.; Gao, G.; Li, C.; Zhang, Z. GEPIA: a web server for cancer and normal gene expression profiling and interactive analyses. *Nucleic acids research* **2017**, *45* (W1), W98−W102.

(17) Chomczynski, P. A reagent for the single-step simultaneous isolation of RNA, DNA and proteins from cell and tissue samples. *Biotechniques* **1993**, *15* (3), 532−534.

(18) Darbankhales, S.; Mirfakhraie, R.; Ghahremani, H.; Asadolahi, M.; Saket-Kisomi, K.; Safakish, L.; Darbeheshti, S.; Ganjkhanlou, Z.; Salami, S.; Sirati-Sabet, M. Effects of Quinacrine on Expression of Hippo signaling Pathway Components (LATS1, LATS2, and YAP) in Human Breast Cancer Stem Cells. *Asian Pacific Journal of Cancer Prevention* **2020**, *21* (11), 3171−3176.

(19) Holderbach, S.; Adam, L.; Jayaram, B.; Wade, R. C.; Mukherjee, G. RASPD+: fast protein-ligand binding free energy prediction using simplified physicochemical features. *Frontiers in molecular biosciences* **2020**, *7*, No. 601065.

(20) Pettersen, E. F.; Goddard, T. D.; Huang, C. C.; Couch, G. S.; Greenblatt, D. M.; Meng, E. C.; Ferrin, T. E. UCSF Chimera—a visualization system for exploratory research and analysis. *Journal of computational chemistry* **2004**, *25* (13), 1605−1612.

(21) Gupta, A.; Gandhimathi, A.; Sharma, P.; Jayaram, B. ParDOCK: an all atom energy based Monte Carlo docking protocol for protein-ligand complexes. *Protein Pept. Lett.* **2007**, *14* (7), 632−646.

(22) Wang, Z.; Pan, H.; Sun, H.; Kang, Y.; Liu, H.; Cao, D.; Hou, T. fastDRH: a webserver to predict and analyze protein−ligand complexes based on molecular docking and MM/PB (GB) SA computation. *Briefings Bioinf.* **2022**, *23* (5), No. bbac201.

(23) Khasraw, M.; Bell, R.; Dang, C. Epirubicin: is it like doxorubicin in breast cancer? *A clinical review. The Breast* **2012**, *21* (2), 142−149.
(24) Hu, J.; Locasale, J. W.; Bielas, J. H.; O'sullivan, J.; Sheahan, K.; Cantley, L. C.; Heiden, M. G. V.; Vitkup, D. Heterogeneity of tumor-induced gene expression changes in the human metabolic network. *Nature biotechnology* **2013**, *31* (6), 522−529.
(25) Shang, M.; Yang, H.; Yang, R.; Chen, T.; Fu, Y.; Li, Y.; Fang, X.; Zhang, K.; Zhang, J.; Li, H. The folate cycle enzyme MTHFD2 induces cancer immune evasion through PD-L1 up-regulation. *Nat. Commun.* **2021**, *12* (1), 1940.
(26) Zhu, Z.; Leung, G. K. K. More than a metabolic enzyme: MTHFD2 as a novel target for anticancer therapy? *Front. Oncol.* **2020**, *10*, 658.
(27) D'Ignazio, L.; Batie, M.; Rocha, S. Hypoxia and inflammation in cancer, focus on HIF and NF-κB. *Biomedicines* **2017**, *5* (2), 21.
(28) Van der Beek, J.; Oosterom, N.; Pieters, R.; de Jonge, R.; Van Den Heuvel-Eibrink, M.; Heil, S. The effect of leucovorin rescue therapy on methotrexate-induced oral mucositis in the treatment of paediatric ALL: A systematic review. *Critical reviews in oncology/hematology* **2019**, *142*, 1−8.
(29) Dalhat, M. H.; Altayb, H. N.; Khan, M. I.; Choudhry, H. Structural insights of human N-acetyltransferase 10 and identification of its potential novel inhibitors. *Sci. Rep.* **2021**, *11* (1), 6051.

https://doi.org/10.1021/acsomega.4c03599
ACS Omega 2024, 9, 44193−44202